

## Magnetic Breakdown at High Fields: Semiclassical and Quantum Treatments

S. Y. Han,<sup>1</sup> J. S. Brooks,<sup>1</sup> and Ju H. Kim<sup>2</sup>

<sup>1</sup>*Physics Department and NHMFL, Florida State University, Tallahassee, Florida 32310*

<sup>2</sup>*Department of Physics, University of North Dakota, P.O. Box 7129, Grand Forks, North Dakota 58202*

(Received 17 December 1999)

The effects of finite temperature and noninteracting spins on magnetic breakdown (MB) in a quasi-two-dimensional organic conductor have been determined by computing the field-dependent free energy using a realistic crystal structure with *no adjustable parameters*. The de Haas–van Alphen oscillation spectra, including the MB phenomena, are thereby obtained microscopically. Within the range of computed magnetic field, from 170 to 1400 T, we find remarkable agreement between the predictions of the semiclassical and quantum treatment. We also find that the Zeeman effect leads to splitting of a frequency corresponding to the fundamental orbit.

PACS numbers: 71.18.+y, 71.20.Rv, 72.15.Gd

High magnetic fields are important for studying magnetic breakdown (MB) and quantum oscillations in low-dimensional materials. A dramatic influence of magnetic field  $B$  on the electronic structure of metals was first elucidated by Hofstadter for a square lattice [1]. A novel feature associated with the field-dependent energy spectrum (i.e., Hofstadter diagram) is that an energy band at  $B = 0$  splits into a series of self-similar patterns of magnetic subbands with increasing field. Such a spectrum, if observed in a real metal, would yield a rich variety of optical, transport, and thermodynamic phenomena due to a complex subband structure. However, for a conventional low-dimensional metal with the lattice constant  $a \approx 1 \text{ \AA}$ , the value of  $B$  for  $\phi/\phi_0 = 1$  is of order 40 000 T, indicating that this property cannot be easily observed. Here  $\phi = Ba^2$  is the magnetic flux through a unit plaquette and  $\phi_0 = hc/e$ . In contrast, the complex subband structures of Hofstadter diagram are, in principle, more accessible in molecular conductors ( $a \approx 10 \text{ \AA}$ ) and in the emerging availability of high magnetic fields [2] which are approaching 1000 T.

In this Letter, the Hofstadter treatment [1] is applied to a BEDT-TTF salt (usually abbreviated as ET) to examine the effect of finite temperature  $T$  and noninteracting spins on MB. We will show that the results from a quantum treatment of MB is surprisingly similar to the semiclassical description based on the Lifshitz-Kosevich (LK) formula with the temperature and spin-dependent damping factors and that the agreement between our calculation and experiments is strikingly good. Furthermore, our calculation predicts the  $B$  dependence of the effective mass due to a nonlinear field dependence of magnetic subbands, and a splitting of a frequency for the fundamental orbit due to the Zeeman effect.

As a point of departure, we consider experimental studies of magnetization in several quasi-two-dimensional organic conductors [3], where the Fermi surface (FS) consists of both a closed (hole) orbit and an open (electron) orbit. In low fields, the closed orbit gives rise to the fundamental frequency  $f_\alpha$ . In sufficiently high fields,

the trajectory of carriers may involve both open and closed orbits as suggested by the semiclassical network picture [4]. This orbit yields the breakdown frequency  $f_\beta$ . In semiclassical theories, the combination frequency  $mf_\beta + nf_\alpha$  along with  $f_\alpha$  and  $f_\beta$  are allowed, but the difference frequency  $f_\beta - f_\alpha$  is explicitly *forbidden* since an abrupt reversal of electron trajectory is not allowed. However, this semiclassically forbidden frequency has been observed. For example, Meyer *et al.* [5] have reported traces of  $f_\beta - f_\alpha$ ,  $f_\beta - 2f_\alpha$ , and  $2f_\beta - 2f_\alpha$  in a fast Fourier transform (FFT) spectrum of the dc magnetization for  $\kappa$ -(ET)<sub>2</sub>Cu(NCS)<sub>2</sub>. Uji *et al.* [6] have seen the peaks corresponding to  $f_\beta - f_\alpha$ ,  $2f_\beta - f_\alpha$ , and  $2f_\beta - 2f_\alpha$  in a FFT spectrum of the same material. Recently, Honold *et al.* [7] observed the frequency corresponding to the difference orbit  $f_\beta - f_\alpha$  in the ac susceptibility of  $\alpha$ -(ET)<sub>2</sub>KHg(SCN)<sub>4</sub>.

These experimental data have stimulated theoretical attempts to explain the origin of the forbidden frequency from a thermodynamic point of view. These attempts include a semiclassical approach using the Pippard network model [8,9], the expanded Landau picture with an independent two-band model [10], and a quantum mechanical approach based on a one-band model with additional inputs to include the MB phenomenon [11]. In contrast, our approach uses the microscopic tight-binding Hamiltonian  $H_{\text{KHg}}$  in Ref. [12] derived for  $\alpha$ -(ET)<sub>2</sub>KHg(SCN)<sub>4</sub> according to the extended Hückel prescription. This material is selected because it is very well studied experimentally, and its nearly square in-plane unit cell can significantly reduce numerical calculations.

A unique aspect of our approach is that both a realistic lattice structure and the Zeeman effect are included in the computation of field-dependent energy bands. Hence, beyond the inclusion of the extended Hückel tight-binding formalism, commonly used to describe the electronic structure of organic conductors, there are *no adjustable parameters*. Four molecular bands obtained by using seven different transfer integrals at  $B = 0$  replicate the electronic structure of the real system [12]. Attempts [13] to study

the effects of spins on the de Haas–van Alphen (dHvA) effect have been made, but to our knowledge, this is the first time the Zeeman effect is included in the Hofstadter spectrum for a realistic crystal structure.

The field-dependent energy spectrum is obtained by introducing magnetic field through the Peierls substitution, for simplicity. We note that the atomic diamagnetism and the field dependence of the transfer integrals can lead to a sizable correction to the energy spectrum when  $\phi/\phi_0 \sim 1$  [14]. However, this correction is negligible in the range of computed magnetic field (170–1400 T). The resulting Hofstadter diagram for  $\alpha$ -(ET)<sub>2</sub>KHg(SCN)<sub>4</sub> is shown in Fig. 1. The symmetry of the energy spectrum, compared to the one-band model [11], is greatly reduced since all four molecular bands are represented in our approach. The number of magnetic subbands and energy gaps for fixed  $B$  depends on the specific values of  $\phi/\phi_0 = p/q$ , where  $p$  and  $q$  are integers, but a mirror symmetry in the energy spectrum about  $\phi/\phi_0 = 1/4$  is due to an artifact of the Peierls substitution. The field-dependent magnetization for  $\phi/\phi_0 < 1/16$  is calculated from the energy spectrum by choosing the canonical ensemble (fixed number of carriers) and by taking the derivative of the free energy with respect to magnetic field. The resulting field-dependent magnetization is shown in Fig. 2. The FFT spectrum of the magnetization yields the relative amplitude of dHvA orbits and shows both allowed and forbidden frequencies, regardless of the use of the canonical or grand canonical ensemble [12]. We now discuss the effect of (i) finite temperature, (ii) magnetic field on effective masses, and (iii) noninteracting spins on MB.

(i) *Finite temperature.*—The effect of finite temperature is included in the free energy through the Fermi function. The thermal broadening effect on the magnetization obtained from the free energy is illustrated in Fig. 2. The FFT amplitude for the fundamental hole orbit  $\alpha$ , the MB

orbit  $\beta$ , and the *forbidden* difference orbit  $\beta - \alpha$  is plotted in Fig. 3 as a function of  $T/B$ , where  $B \approx 310$  T is the inverse of the average  $\phi_0/\phi$  for the FFT spectrum in Fig. 2. The dotted lines in Fig. 3 represent the semiclassical LK treatment [15] of the dHvA amplitudes obtained by using the damping factor

$$R_T = (\ell X T m^*/m_e B) / \sinh(\ell X T m^*/m_e B), \quad (1)$$

which describes the phase smearing effect in quantum oscillations at finite  $T$ . Here  $\ell$  is a harmonic number,  $X = \pi^2 k_B / \mu_B = 14.69$  T/K,  $\mu_B$  is the Bohr magneton,  $m^*$  is the effective cyclotron mass, and  $m_e$  is the electron mass. The effective mass parameter  $m^*/m_e$  for each orbit, as obtained by fitting our numerical results to Eq. (1), is tabulated in Table I. Considering the range of magnetic field used in the calculation, the computed values for the frequencies and  $m^*/m_e$  are in remarkable agreement with the experimental values [2,6,7,16,17]. We note that the effective masses for higher harmonics of both the  $\alpha$  and  $\beta$  orbit were smaller than the one obtained by using the simple prescription of  $m_\ell^* \approx \ell m^*$ . This appears to be the case for both our calculation and experiments.

(ii) *Magnetic field dependence.*—Another result of the calculation is that both the effective mass [Fig. 4(a)] and the amplitude of dHvA orbits [Fig. 4(b)] depend on magnetic field. The effective mass of the fundamental ( $m_\alpha^*$ ) and the MB ( $m_\beta^*$ ) orbit, *derived from the LK analysis of our result*, increases slightly and decreases rapidly with magnetic field, respectively.  $m_\alpha^*$  is consistent with a suggestion that  $m^*$  increases with  $B$  due to the nonlinear field dependence of magnetic subbands [18]. The origin of the field dependence for  $m_\beta^*$  is difficult to visualize directly since the electron orbit involves both a closed and an open FS, but the drastic decrease in  $m_\beta^*$  with field is certainly a manifestation of the MB system. These behaviors represent a deviation from the expectations of the standard LK theory, where the energy spectrum depends linearly on  $B$

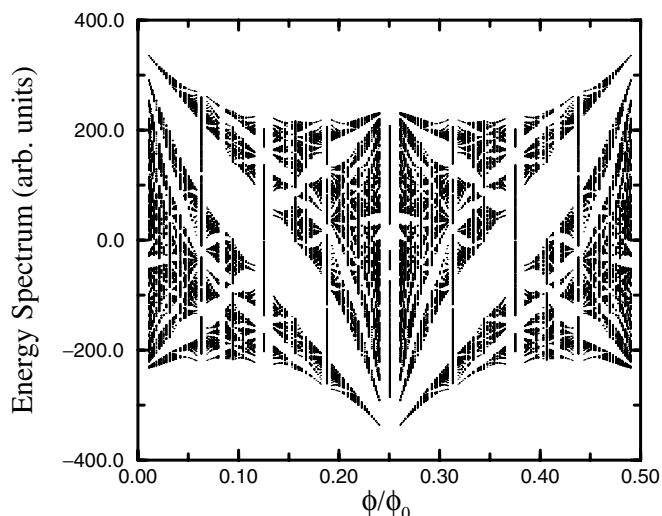


FIG. 1. The Hofstadter diagram for the quasi-two-dimensional organic conductor  $\alpha$ -(ET)<sub>2</sub>KHg(SCN)<sub>4</sub>.

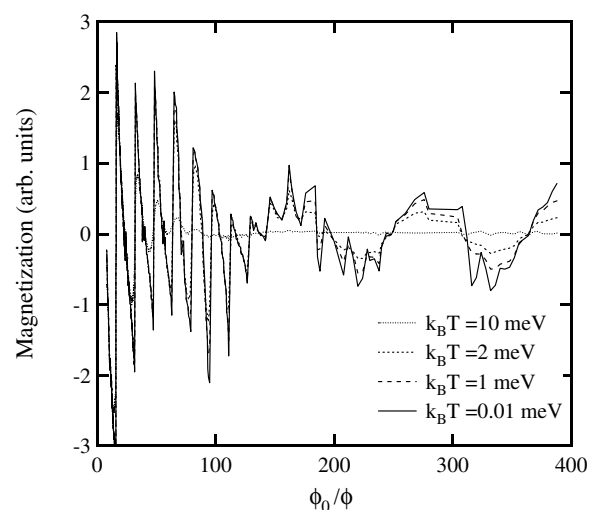


FIG. 2. The magnetization versus inverse magnetic field for  $k_B T = 0.01, 1, 2, 10$  meV.

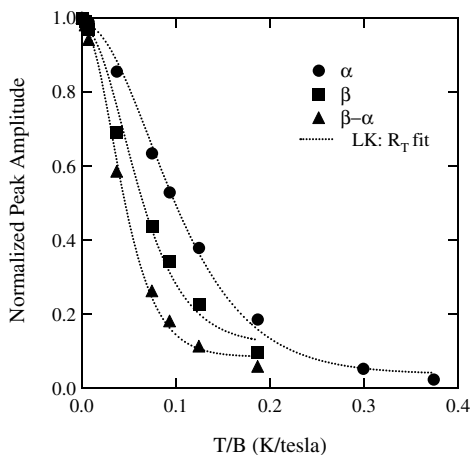


FIG. 3. The normalized FFT amplitude versus  $T/B$  for  $f_\alpha$  (filled circles),  $f_\beta$  (filled squares), and  $f_\beta - f_\alpha$  (filled triangles). The field range used in this analysis is  $170 \leq B \leq 1400$  T. The dotted lines are fits using  $R_T$ .

and where no MB occurs. As shown in Fig. 1, the field dependence of magnetic subbands is nonlinear, and this deviation becomes stronger with increasing field. Field-dependent effective mass effects have been reported in experiments in pulsed magnetic fields (of order 50 T) for both magnetization and transport studies [19]. A direct comparison with our predictions must be made with caution since our field range is significantly higher. Also, application of the LK theory to highly nonsinusoidal wave forms, as observed in the transport studies, can induce artifacts into the mass analysis. The FFT amplitude shown in Fig. 4(b) indicates that the dHvA amplitude of the  $\alpha$  orbit for  $B > B_c \approx 265$  T (the estimated breakdown field) [12] decreases with the field, but the amplitude of the  $\beta$  orbit, its second harmonic, and the  $\beta - \alpha$  orbit increase gradually with the field. Figures 4(a) and 4(b) also indicate that the present quantum treatment of MB should be distinguished from the approaches based on an independent multiple-band model [10] since the interdependence between electrons in different molecular bands cannot be accounted for in these models.

(iii) *Noninteracting spin effects.*—The effect of noninteracting spins on MB is determined by adding the Zeeman term  $H_s = \sigma g_e \mu_B B/2$  to the Hamiltonian  $H_{KHg}$  in the calculation of field-dependent energy spectrum. Here,  $\sigma = \pm 1$ , and  $g_e$  is the electron  $g$ -factor. For noninteracting spins, the spin states are orthogonal to other eigenstates. As a result, the spin-dependent terms appear

TABLE I. Numerically computed frequency and the effective mass for the  $\alpha$ ,  $\beta$ , and  $\beta - \alpha$  orbits are compared with the values obtained from the dHvA effect data.

	Frequency (T)		$m^*/m_e$		Refs.
	Theory	Expt.	Theory	Expt.	
$\alpha$	680	670	$1.53 \pm 0.04$	1.65, 1.85	[2,6]
$\beta$	4080	4260	$2.48 \pm 0.20$	$3.3 \pm 0.5, 3.5$	[7,17]
$\beta - \alpha$	3400	...	$3.41 \pm 0.16$	...	...

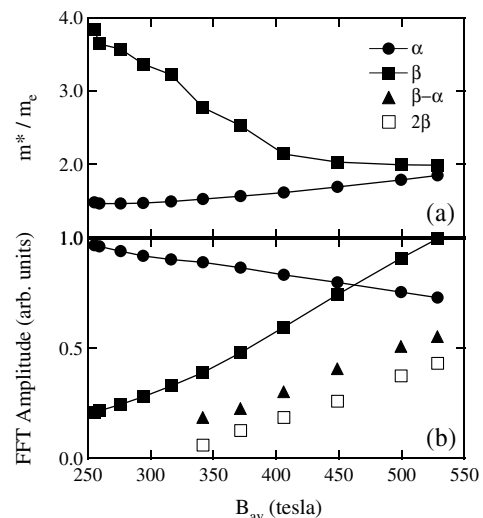


FIG. 4. (a)  $m^*/m_e$  and (b) the FFT amplitude of the dHvA orbits determined from the magnetization shown in Fig. 2. Here  $B_{av}$  is the average magnetic field for the FFT with a width  $\delta(\phi_0/\phi) = 240$ .

as diagonal elements in a matrix representation of the Hamiltonian [12]. The FFT spectrum of magnetization for the  $g$ -factor ranging from  $g_e = 0-3$  (in intervals of 0.1) is shown in Fig. 5. Here we choose  $k_B T = 0.002$  meV. Inclusion of the spin effect in the Hofstadter spectrum yields a new result: *the Zeeman effect leads to splitting of the fundamental frequency.* A peak corresponding to  $f_\alpha = 680$  T splits into two peaks with  $f_{\alpha,1} = 480$  T and  $f_{\alpha,2} = 750$  T for a nonzero value of  $g_e$  but becomes clearly visible for  $g_e > 2.1$  due to the increase in the spectral weight. This splitting may be due to the nonlinear field dependence of magnetic subbands,

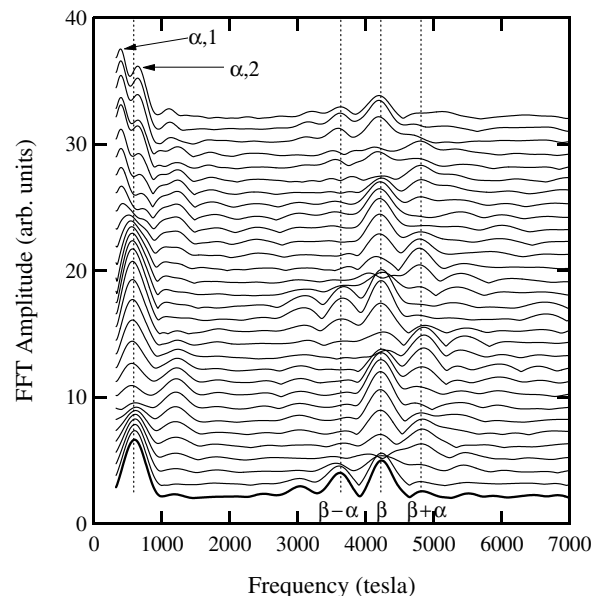


FIG. 5. The FFT spectra for  $g_e$  between 0 and 3 are plotted in an interval of 0.1. The curves are vertically offset in proportion to  $g_e$  for clarity.

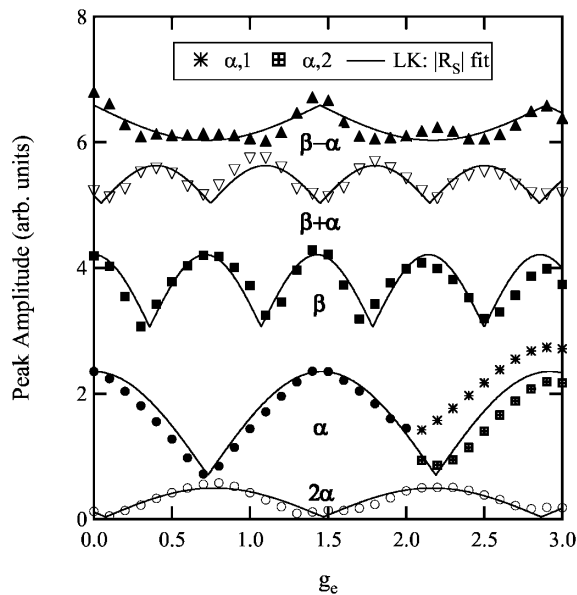


FIG. 6. The FFT amplitude versus  $g_e$  for  $f_\alpha$  (filled circles),  $2f_\alpha$  (open circles),  $f_\beta$  (filled squares),  $f_{\beta+\alpha}$  (open triangles), and  $f_{\beta-\alpha}$  (filled triangles). The solid lines are fits using  $R_s$ . The curves are offset for clarity. A split of  $f_\alpha$  into  $f_{\alpha,1}$  and  $f_{\alpha,2}$  becomes clearly visible for  $g_e > 2.1$ .

indicating a complex interplay between spin-up and spin-down magnetic subbands with magnetic field. Splitting of  $f_\beta$  and  $f_{\beta-\alpha}$  may also occur when  $g_e$  is nonzero, but this has not been observed yet, probably due to a limitation in the resolution of our calculations. We note that House *et al.* [16] reported the appearance of other frequencies, which may be related to  $f_{\alpha,1}$  and  $f_{\alpha,2}$ , near the fundamental frequency in the measurements of angle-dependent magnetoresistance. However, the experimental data is inconclusive, suggesting the need for further investigation. The FFT amplitudes of each frequency plotted in Fig. 6 show a nonmonotonic dependence on  $g_e$  due to the band crossing between spin-up and spin-down magnetic subbands. Here, the result of our calculation is compared with the semiclassical LK treatment (solid lines) of the spin effect in terms of the damping factor

$$R_s \approx \cos(p\pi g_e m^*/2m_e). \quad (2)$$

It is evident from the figure that the cosine behavior which is expected from the LK treatment is clearly seen in the field-dependent energy spectrum when the Zeeman effect is included. Similar to the estimation of  $m^*$  by using  $R_T$  of Eq. (1), the effective mass can also be determined by fitting our numerical result with  $R_s$ . The effective masses of  $m_\alpha^*/m_e \approx 1.4$  and  $m_\beta^*/m_e \approx 2.8$  obtained by using  $|R_s|$  are in close agreement with those determined by fitting with  $R_T$ , as shown in Table I.

In summary, we have determined the effect of finite temperature and noninteracting spin by examining MB in  $\alpha$ -(ET)<sub>2</sub>KHg(SCN)<sub>4</sub>, using a microscopic model with *no adjustable parameters* which yields the quantum oscilla-

tion frequencies for the  $\alpha$ ,  $\beta$ , and  $\beta - \alpha$  orbits, as observed in thermodynamic (magnetization) experiments. By applying the conventional theory of magneto-oscillations (i.e., the LK formalism) to our numerical result, we obtained  $m^*/m_e$  for the dHvA orbits that are in close agreement with the experimental values. Perhaps, this looks surprising since the present limit of magnetic field in experiments is about 60 T, whereas the range of  $B$  in our computation is from 170 to 1400 T. However, this correspondence is quite reasonable since the ratio  $B/T$  (of order 10 T/K for both the computational and experimental regimes of Table I) enters the LK damping factor. In our quantum treatment of MB, we found that (i)  $m^*/m_e$  of the dHvA orbits depends on magnetic field for  $B > 250$  T and (ii) the fundamental frequency splits into two due to the Zeeman effect. These results are a consequence of interplay between the molecular bands near the Fermi energy and the nonlinear field dependence of magnetic subbands which are included naturally in the Hofstadter diagram for a realistic electronic structure.

We acknowledge support from NSF-DMR 95-10427 and 99-71474 (J.S.B.) and ND EPSCOR through NSF Grant No. EPS-9874802 (J.H.K.). The NHMFL is supported through a cooperative agreement between the state of Florida and the NSF through NSF-DMR-95-27035.

- [1] D. R. Hofstadter, *Phys. Rev. B* **14**, 2239 (1976).
- [2] J. S. Brooks *et al.*, *Physica (Amsterdam)* **246B-247B**, 319 (1998).
- [3] T. Ishiguro, K. Yamaji, and G. Sato, *Organic Superconductors* (Springer-Verlag, Berlin, 1998).
- [4] A. B. Pippard, *Proc. R. Soc. London A* **270**, 1 (1962).
- [5] F. A. Meyer *et al.*, *Europhys. Lett.* **32**, 681 (1995).
- [6] S. Uji *et al.*, *Solid State Commun.* **100**, 825 (1996).
- [7] M. M. Honold *et al.*, *Phys. Rev. B* **58**, 7560 (1998).
- [8] N. Harrison *et al.*, *J. Phys. Condens. Matter* **8**, 5415 (1996).
- [9] J. Fortin and T. Ziman, *Phys. Rev. Lett.* **80**, 3117 (1998).
- [10] A. Alexandrov and A. Bratkovsky, *Phys. Rev. Lett.* **76**, 1308 (1996); M. Nakano, *J. Phys. Soc. Jpn.* **66**, 19 (1997).
- [11] K. Machida, K. Kishigi, and Y. Hori, *Phys. Rev. B* **51**, 8946 (1995).
- [12] J. H. Kim, S. Y. Han, and J. S. Brooks, *Phys. Rev. B* **60**, 3213 (1999).
- [13] M. A. Itskovsky *et al.*, *Phys. Rev. B* **58**, R13347 (1998); K. Kishigi *et al.* (unpublished).
- [14] A. Alexandrov and H. Capellmann, *Phys. Rev. Lett.* **66**, 365 (1991); V. N. Nicopoulos and S. A. Trugman, *Phys. Rev. Lett.* **64**, 237 (1990).
- [15] I. M. Lifshitz and A. M. Kosevich, *Zh. Eksp. Teor. Fiz.* **29**, 730 (1955); D. Shoenberg, *Magnetic Oscillations in Metal* (Cambridge University Press, Cambridge, England, 1984).
- [16] A. A. House *et al.*, *J. Phys. Condens. Matter* **8**, 10361 (1996); **8**, 10377 (1996).
- [17] J. Caulfield *et al.*, *Phys. Rev. B* **51**, 8325 (1995).
- [18] J. H. Kim and I. Vagner, *Phys. Rev. B* **48**, 16564 (1993).
- [19] N. Harrison *et al.*, *Phys. Rev. B* **58**, 10248 (1998); V. N. Laukhin *et al.*, *Physica (Amsterdam)* **211B**, 282 (1995).